Fractional Order Sliding Mode Control via Disturbance Observer for a Class of Fractional Order Systems With Mismatched Disturbance

Article *in* SSRN Electronic Journal · January 2018

DOI: 10.2139/ssrn.3281368

CITATIONS
0

READS
38

3 authors, including:

Jing Wang
Beijing University of Chemical Technology
76 PUBLICATIONS **204** CITATIONS

SEE PROFILE

YangQuan Chen
University of California, Merced
908 PUBLICATIONS **23,795** CITATIONS

SEE PROFILE

Mechatronics 53 (2018) 8–19

Contents lists available at ScienceDirect

Mechatronics

journal homepage: www.elsevier.com/locate/mechatronics

Fractional order sliding mode control via disturbance observer for a class of fractional order systems with mismatched disturbance,☆,☆☆

Jing Wang*,[a], Changfeng Shao[a], Yang-Quan Chen[b]

[a] College of Information Science & Technology, Beijing University of Chemical Technology, Beijing 100029, China
[b] Mechatronics, Embedded Systems and Automation Lab, School of Engineering, University of California, Merced, CA 95343, USA

ARTICLE INFO

MSC:
00-01
99-00

Keywords:
Fractional order calculus
Fractional order sliding mode control
Fractional order disturbance observer
Mismatched uncertain

ABSTRACT

This article proposes a novel fractional order sliding mode control for a class of fractional order and integer order systems with mismatched disturbances. First, a new fractional order disturbance observer is designed to estimate the fractional order differential of the mismatched disturbance directly. Second, the fractional order sliding surface and controller are proposed based on the designed disturbance observer. Our method can deal with mismatched disturbance and has better control performance with faster response speed, lower overshoot, and less chattering effect. The simulations on Quad–Rotor UAV and Maglev suspension systems demonstrate the effectiveness of the proposed method.

1. Introduction

Fractional calculus is a powerful method to describe data memory and heredity. It has the property of history dependence and long range correlation. It is the generalization of classical integer order calculus. It can describe some real systems more accurately than the traditional integer order method. Researchers have gradually found that fractional order calculus can characterize some non-classical phenomena in natural sciences and engineering applications. The theory of fractional calculus has been successfully applied in biology, physics, chemistry, automatic control, materials science, engineering, etc. [1,2]. As an important tool to improve the control performance, fractional calculus combines with many traditional control schemes, such as fractional order PID control [3], fractional order adaptive control [4], fractional order optimal control [5] and fractional order sliding mode control [6–8].

In real life, uncertainty and external disturbance often exist in the actual systems. External disturbances can be divided into two types: matching disturbances and mismatched disturbances. It is an important task to control the system and judge the stability of the system with mismatched disturbance. Sliding mode control (SMC) is an effective robust control method to deal with external disturbance. Several improved SMC methods have been proposed based on linear matrix inequality (LMI) [9], Riccati approach [10], adaptive technique [11], and neural network [12]. Integral sliding mode control (I-SMC) designs an integral sliding surface for a class of nonlinear fractional order systems [13,14], furthermore an improved stable sliding surface is given in [15]. Yet the closed-loop stability is not proven in these literatures. Lately the closed-loop stability is proven via the indirect Lyapunov method [16]. In I-SMC, a high-frequency switching gain is designed to force the states arrive the integral sliding surface. However, in the case of mismatched disturbances, I-SMC method can make states reach the desired equilibrium on the sliding surface. But at the same time, the I-SMC method may bring some adverse effects to the systems, such as large overshoot and long settling time. It is reported that the I-SMC method is applied to various systems [17,18].

When integer order SMC methods is used to deal with fractional order system, they always reject the disturbances in a robust way, but chattering is a serious problem that needs to be solved. [19–21] consider the chattering free control to avoid the serious chattering phenomenon in SMC. Kim [22] proposes a novel switching surface and a robust fractional control law. Subsequently, the sign function of the control input is transferred into the fractional derivative of the control signal in order to avoid the chattering. A new dynamic PID-SMC for a class of uncertain nonlinear systems is proposed and an adaptive parameter tuning method is used to estimate the unknown upper bounds of the disturbances [21]. This approach can eliminate the chattering phenomenon caused by the switching control action and

☆ This paper was recommended for publication by Associate Editor Prof. Hamid Reza Karimi.

☆☆ This work is supported by the National Natural Science Foundation of China (No. 61573050) and the open-project grant funded bythe State Key Laboratory of Synthetical Automation for Process Industry at the Northeastern University (No. PAL-N201702)

* Corresponding author.
E-mail address: jwang@mail.buct.edu.cn (J. Wang).

https://doi.org/10.1016/j.mechatronics.2018.05.006
Received 13 December 2017; Received in revised form 28 March 2018; Accepted 12 May 2018

realize high-precision performance.

Moreover, the disturbance observer (DOB) technique is also used to counteract the mismatched uncertainties and reduce chattering in the systems [22–25]. Yang et al. [26] proposes a disturbance observer based sliding mode control approach for systems with mismatched uncertainties. Li et al. [27] designs a sliding mode control based on nonlinear disturbance observer to counteract the mismatch disturbance and reduce the chattering. Zhang et al. [28] develops a disturbance observer -based integral sliding-mode control approach for continuous-time linear systems with mismatched disturbances. The disturbance observer is used to get the estimation of the disturbance, and the result can be incorporated in the controller to counteract the disturbance.

Considering the advantages of fractional order calculus, the fractional order is incorporated into the design of sliding mode control, which can improve the chattering problem and speed up the response of the closed-loop system. Wei proposed an adaptive backstepping output feedback control for a class of nonlinear fractional order systems [29]. In [30], the fractional order sliding mode control (FOSMC) for a single link flexible manipulator is realized. The control law of the proposed FOSMC scheme is designed using Lyapunov stability analysis. It has better control performance and is robust to external load disturbance and parameter variations. However, there is little research effort to combine FOSMC with fractional order disturbance observer, and then apply it to fractional order dynamic systems with mismatched disturbances. Pashaei and Badamchizadeh [31] tries to design a new FOSMC based on a nonlinear disturbance observer that exhibits better control performance, such as fast and robust stability, the disturbance and chartering rejection.

In this paper, we propose a new fractional order disturbance observer. It can estimate the fractional order derivative of the disturbance directly. The estimation of unmatched disturbance can be used to design sliding mode control law more conveniently. Subsequently, we designed a new fractional order siding mode control via a fractional order disturbance observer. The proposed FOSMC is generally applicable for both fractional order systems and integer order systems. The proposed method also shows good control performance and reduces the system chattering.

The main contributions of the paper are as follows. A new fractional order disturbance observer is proposed to estimate the mismatch disturbance and the estimation error is upper bounded. The main advantage is that it can get the fractional order of the mismatch disturbance directly. Based on the proposed DOB, a novel FOSMC method is proposed. It has better performances in weakening tracking error and chattering effect, compared with the traditional sliding mode control. The proposed FOSMC-DOB has less overshoot and faster convergence speed. Moreover, the proposed FOSMC-DOB is applicable not only for fractional order systems but also for integer order systems. In order to verify the excellent properties of the proposed FOSMC-DOB, a Quad-Rotor UAV system with integer order and a Maglev suspension system with fractional order are given. The proposed method shows good control performance in these systems. It can decrease the tracking error with a high rate of speed and weak chattering. Moreover, the FOSMC-DOB is not sensitive with controller parameters.

This paper is structured as follows. Section 2 gives the basic definitions of fractional calculus, the description of integer order and fractional order system. Section 3 contains two parts, one is the design of the fractional order DOB, and another is the design of FOSMC. Section 4 shows the experimental results for two different actual system. Finally, the conclusions are drawn in Section 5.

2. Basic knowledge and problem formulation

2.1. Basic definitions of fractional calculus

There are several definitions for fractional order derivatives [32], and three most commonly used definitions are the Grünwald–Letnikov's, Riemann–Liouville's, and Caputo's derivative definitions. In this paper, we use the Riemann–Liouville's definition.

Definition 1. The Riemann–Liouville fractional integral of α order of a continuous function $f(t)$ is defined as,

$$ {}_RD^{-\alpha}f(t) = \frac{1}{\Gamma(\alpha)}\int_{t_0}^{t}(t-\tau)^{\alpha-1}f(\tau)\mathrm{d}\tau, \quad t > t_0, \quad \alpha \in R^+, \tag{1}$$

where m is the largest positive integer number satisfying the following condition $m-1 < \alpha < m$. Γ is the Gamma function, which is defined as following,

$$\Gamma(q) = \int_0^{\infty} x^{q-1}e^{-x}dx. \tag{2}$$

Definition 2. The Riemann–Liouville fractional derivative of α order of a continuous function $f(t)$ is defined as,

$$ {}_RD^{\alpha}f(t) = \frac{d^m}{dt^m}\left[\frac{1}{\Gamma(m-\alpha)}\int_{t_0}^{t}\frac{f(\tau)}{(t-\tau)^{\alpha-m+1}}d\tau\right]. \tag{3}$$

It should be noted that the fractional integral of order $\alpha > 0$ is represented by $D^{-\alpha}$.

Property 1. For $\alpha = n$, where n is an integer, the operation $D_t^{\alpha}f(t)$ is the same as the integer order calculus, i.e., $D_t^n f(t) = \frac{d^n}{dt^n}f(t)$, and also for α=0, we have $D_t^0 f(t) = \frac{d^0}{dt^0}f(t) = f(t)$.

Property 2. The fractional order integration or differentiation calculus are linear operations, which is similar to the integer order calculus,

$$D_t^{\alpha}(\lambda f(t) + \mu g(t)) = \lambda D_t^{\alpha}f(t) + \mu D_t^{\alpha}g(t). \tag{4}$$

Property 3 ([33]). For the arbitrary fractional order, $\alpha > 0$, $\beta > 0$, $\beta \in (m-1, m)$, the following equalities hold for the hybrid fractional derivative and integral operation,

$$D_t^{\alpha}(D_t^{\beta}f(t)) = D_t^{\alpha+\beta}f(t), \tag{5}$$

$$D_t^{\alpha}(D_t^{-\beta}f(t)) = D_t^{\alpha-\beta}f(t), \tag{6}$$

$$D_t^{-\alpha}(D_t^{\beta}f(t)) = D_t^{-\alpha+\beta}f(t) - \sum_{j=1}^{m}[D_t^{\beta-j}f(t)]_{t=t_0}\frac{(t-t_0)^{\alpha-j}}{\Gamma(1+\alpha-j)}, \tag{7}$$

and $D_t^{\beta\cdot j}f(t)$ *are bounded at* $t = t_0$.

Property 4 ([33]). The fractional derivative operator $D_t^{\alpha}f(t)$ commutes with $\frac{d^n}{dt^n}f(t)$, i.e., that

$$D^m(D^{\alpha}f(t)) = D^{\alpha+m}f(t) \tag{8}$$

only if at the lower terminal $t = t_0$ of the fractional differentiation the function $f(t)$ satisfies the conditions

$$f^{(s)}(t_0) = 0(s = 0, 1, \ldots, m-1). \tag{9}$$

Lemma 1 ([19]). *For an integrable function* $f(t)$, *if there is at least one* $t_1 \in (0, t)$ *such that* $f(t_1) \neq 0$, *then there is a positive constant* N *such that* $D^{-\alpha}|f(t)| \geq N$.

2.2. Problem formulation

Consider a general dynamical system with mismatched external disturbances,

$$\begin{cases} D^{\beta}x(t) = Ax(t) + Bu(t) + B_d d(t) \\ y(t) = Cx(t) \end{cases}, \tag{10}$$

where $\beta \in (0, 1]$ is the order of the system, $x(t) \in R^n$ is the state variable, $u(t) \in R^m$ is the control signal, $y(t) \in R^p$ is the output and $d(t) \in R^1$ is the mismatched external disturbance. $A \in R^{n\times n}$ is the state matrix. $B \in R^{n\times m}$ is the control matrix. $B_d \in R^{n\times 1}$ is the disturbance matrix. $C \in R^{p\times n}$ is the output matrix. System (10) describes a fractional-order

dynamic system when $\beta \in 0$, 1, and if $\beta = 1$, it reduces into a class of integer order systems,

$$\begin{cases} \dot{x}(t) = Ax(t) + Bu(t) + B_d d(t) \\ y(t) = Cx(t) \end{cases} \tag{11}$$

Assumption 1. The mismatched disturbance $d(t)$ is bounded, $\|d(t)\| \le \varepsilon$, where ε is a positive constant.

We argue that little benefit can be gained from using advanced control technique such as DOB, if $d(t)$ is a white noise. For the general fractional/integer-order systems (10) with mismatched disturbances, the designed controller $u(t)$ is to make the output asymptotically tracking the desired reference $y_d(t)$ in finite time, and the tracking error approaching to zero without any effect from the external mismatched disturbances.

3. Design of fractional order sliding mode control

The SMC has high robustness in restraining the matched disturbances. The traditional SMC method is not effective to deal with system (10) that contains the mismatched disturbances. So we present a fractional order disturbance observer to estimate the mismatched disturbance, then design a improved FOSMC based on it.

3.1. Fractional order disturbance observer

As we know, the integer order disturbance observer defined as following always is used to estimate the disturbance $d(t)$ [22,23],

$$\begin{cases} \dot{p}(t) = -LB_d(p(t) + Lx(t)) - L(Ax(t) + Bu(t)) \\ \hat{d}(t) = p(t) + Lx(t) \end{cases}, \tag{12}$$

where $\hat{d}(t)$ is the estimation of the disturbance $d(t)$, $p(t)$ and L are the auxiliary vector and the gain matrix of the observer, respectively. The design of L should satisfy that $-LB_d$ is Hurwitz.

The limitation of the traditional integer order disturbance observer is that we can not obtain any information about the fractional order derivative of the disturbance $d(t)$ except its estimation. So a new fractional order disturbance observer should be designed to directly get the fractional order derivative of $d(t)$ as following,

$$\begin{cases} D^{1+\alpha-\beta}p(t) = -LB_d(D^{\alpha-\beta}p(t) + LD^{\alpha-1}x(t)) \\ \qquad\qquad - L(AD^{\alpha-\beta}x(t) + BD^{\alpha-\beta}u(t)), \\ D^{1+\alpha-\beta}\hat{d}(t) = D^{1+\alpha-\beta}p(t) + LD^{\alpha}x(t) \end{cases} \tag{13}$$

where $\hat{d}(t)$ is the estimation of the disturbance $d(t)$, $p(t)$ is the auxiliary vector of the observer, L is the gain matrix of the observer, and $\alpha \in (0, \beta)$ depends on the order of FOSMC which is to be designed in Section 3.2.

The estimation error of $d(t)$ is

$$e_d(t) = d(t) - \hat{d}(t). \tag{14}$$

The fractional order calculus of $e_d(t)$ is

$$D^{1+\alpha-\beta}e_d(t) = D^{1+\alpha-\beta}d(t) - D^{1+\alpha-\beta}\hat{d}(t). \tag{15}$$

Lemma 2 ([34]). *Assume A is Hurwitz and has n distinct eigenvalues. Let X be a nonsingular matrix such that $XAX^{-1} = \mathrm{diag}(\lambda_1, \ldots \lambda_n)$. There exist an positive constant σ such that*

$$\|e^{At}\| \le \sigma e^{\lambda_{\max}(A)t}, \tag{16}$$

where $\sigma = \|X^{-1}\|\|X\|$.

Lemma 3. *For the proposed fractional order disturbance observer (13), $D^{1+\alpha-\beta}e_d(t)$ is bounded and satisfies*

$$\|D^{1+\alpha-\beta}e_d(t)\| \le \zeta, \tag{17}$$

where ζ is a positive scalar.

Proof. According to (13), (15) and property 4, we have,

$$\begin{aligned} &\frac{d(D^{1+\alpha-\beta}e_d(t))}{dt} \\ &= D^{2+\alpha-\beta}d(t) - D^{2+\alpha-\beta}\hat{d}(t) \\ &= D^{2+\alpha-\beta}d(t) - D^{2+\alpha-\beta}p(t) - LD^{1+\alpha}x(t) \\ &= D^{1+\alpha-\beta}\dot{d}(t) - D^{2+\alpha-\beta}p(t) - LD^{1+\alpha-\beta}(D^{\beta}x(t)). \end{aligned} \tag{18}$$

Substitute the system (10) into (18),

$$\begin{aligned} &\frac{d(D^{1+\alpha-\beta}e_d(t))}{dt} \\ &= D^{1+\alpha-\beta}\dot{d}(t) - D^{2+\alpha-\beta}p(t) - L(AD^{1+\alpha-\beta}x(t) + BD^{1+\alpha-\beta}u(t) + B_dD^{1+\alpha-\beta}d(t)) \\ &= D^{1+\alpha-\beta}\dot{d}(t) + LB_d(D^{1+\alpha-\beta}p(t) + LD^{\alpha}x(t)) + L(AD^{1+\alpha-\beta}x(t) + BD^{1+\alpha-\beta}u(t)) \\ &- L(AD^{1+\alpha-\beta}x(t) + BD^{1+\alpha-\beta}u(t) + B_dD^{1+\alpha-\beta}d(t)) \\ &= D^{1+\alpha-\beta}\dot{d}(t) + LB_dD^{1+\alpha-\beta}\hat{d}(t) - LB_dD^{1+\alpha-\beta}d(t) \\ &= D^{1+\alpha-\beta}\dot{d}(t) - LB_dD^{1+\alpha-\beta}e_d(t). \end{aligned} \tag{19}$$

Define $M = -LB_d$, and $d_{\mathrm{new}}(t) = D^{1+\alpha-\beta}d(t)$, so $e_{d_{\mathrm{new}}}(t) = D^{1+\alpha-\beta}e_d(t)$, then (19) can be written as

$$\dot{e}_{d_{\mathrm{new}}}(t) = \dot{d}_{\mathrm{new}}(t) + Me_{d_{\mathrm{new}}}(t). \tag{20}$$

Taking the integration of (20) gives

$$e_{d_{\mathrm{new}}}(t) = e^{Mt}e_{d_{\mathrm{new}}}(0) + \int_0^t e^{M(t-\tau)}M\dot{d}_{\mathrm{new}}(\tau)\mathrm{d}\tau. \tag{21}$$

Based on Riemann–Liouville's derivative definition and Assumption 1,

$$\begin{aligned} \|d_{\mathrm{new}}(t)\| &= \|D^{1+\alpha-\beta}d(t)\| \\ &= \left\| \frac{d}{dt}\left[\frac{1}{\Gamma(\beta-\alpha)} \int_0^t (t-\tau)^{-1-\alpha+\beta}d(\tau)d\tau \right] \right\| \\ &= \left\| \frac{1}{\Gamma(\beta-\alpha)} \int_0^t (-1-\alpha+\beta)(t-\tau)^{-2-\alpha+\beta}d(\tau)d\tau \right\| \\ &\le \left\| \frac{1}{\Gamma(\beta-\alpha)} \right\| \|d(t)\| \left\| \int_0^t (-1-\alpha+\beta)(t-\tau)^{-2-\alpha+\beta}d\tau \right\| \\ &= \left\| \frac{\varepsilon(-1-\alpha+\beta)}{\Gamma(\beta-\alpha)} \right\| \left\| \int_0^t (t-\tau)^{-2-\alpha+\beta}d\tau \right\|. \end{aligned} \tag{22}$$

Define $\delta = \|\frac{\varepsilon(-1-\alpha+\beta)}{\Gamma(\beta-\alpha)}\| \|\int_0^t (t-\tau)^{-2-\alpha+\beta}d\tau\|$, where δ is a positive scalar. Thus we have $\|d_{\mathrm{new}}(t)\| \le \delta$.

Then

$$\begin{aligned} &\|e_{d_{\mathrm{new}}}(t)\| \\ &\le \|e^{Mt}e_{d_{\mathrm{new}}}(0)\| + \left\| \int_0^t e^{M(t-\tau)}\dot{d}_{\mathrm{new}}(\tau)\mathrm{d}\tau \right\| \\ &\le \|e^{Mt}\|\|e_{d_{\mathrm{new}}}(0)\| + \left\| e^{M(t-\tau)}d_{\mathrm{new}}(\tau)|_0^t + M\int_0^t e^{M(t-\tau)}d_{\mathrm{new}}(\tau)\mathrm{d}\tau \right\| \\ &\le \sigma e^{\lambda_{\max}(M)t}\|e_{d_{\mathrm{new}}}(0)\| + \Bigg\| \|d_{\mathrm{new}}(t) - e^{Mt}d_{\mathrm{new}}(0)\| \\ &\quad + M\int_0^t \|e^{M(t-\tau)}\|\|d_{\mathrm{new}}(\tau)\|\mathrm{d}\tau \Bigg\| \\ &\le \sigma e^{\lambda_{\max}(M)t}\|e_{d_{\mathrm{new}}}(0)\| + \Bigg\| \|d_{\mathrm{new}}(t)\| + \|e^{Mt}d_{\mathrm{new}}(0)\| \\ &\quad + M\sigma\delta\int_0^t \|e^{\lambda_{\max}(M)(t-\tau)}\|\mathrm{d}\tau \Bigg\| \\ &\le \sigma e^{\lambda_{\max}(M)t}\|e_{d_{\mathrm{new}}}(0)\| + \left\| \delta + \|e^{Mt}d_{\mathrm{new}}(0)\| \right. \\ &\quad \left. + M\sigma\delta\frac{1}{\lambda_{\max}(M)}\left(e^{\lambda_{\max}(M)t} - 1\right) \right\|. \end{aligned} \tag{23}$$

M is Hurwitz matrix, so $\mathrm{Re}\,\lambda_{\max}(M) < 0$, $e^{\lambda_{\max}(M)t} \le 1$.
Then

$$\begin{aligned}\|e_{d_{\text{new}}}(t)\| &\le \sigma\|e_{d_{\text{new}}}(0)\| + \delta + \|d_{\text{new}}(0)\| \\ &\quad + \left\| M\sigma\delta\frac{1}{\lambda_{\max}(M)}\left(e^{\lambda_{\max}(M)t} - 1\right)\right\| \\ &\le \sigma\|e_{d_{\text{new}}}(0)\| + \delta + \|d_{\text{new}}(0)\| + \left\| M\sigma\delta\frac{1}{\lambda_{\max}(M)}\right\| \end{aligned} \tag{24}$$

Define $\zeta{=}\sigma\|e_{d_{\text{new}}}(0)\| + \delta + \|d_{\text{new}}(0)\| - M\sigma\delta\frac{1}{\lambda_{\max}(M)}$ and take it into (24), the (17) can be immediately obtained. □

Consider the integer order system (11), the disturbance observer (13) transfers to

$$\begin{cases} D^{1+\alpha}p(t) = -LB_d(D^\alpha p(t) + LD^\alpha x(t)) - L(AD^\alpha x(t) + BD^\alpha u(t)) \\ D^\alpha\hat{d}\,(t) = D^\alpha p(t) + D^\alpha Lx(t) \end{cases} \tag{25}$$

Corollary 1. *Towards the disturbance observer (25) for integer order system (11), $D^\alpha e_d(t)$ satisfies the following inequality*

$$\|D^\alpha e_d(t)\| \le \xi, \tag{26}$$

where ξ is a positive scalar.

The integer order system can be viewed as a special case of the fractional order case. Thus the proof of Corollary 1 can be omitted.

3.2. Fractional order sliding mode control

In this section, a novel fractional order sliding mode control is proposed for the systems with mismatched disturbances.

Assuming that the target value of the output $y(t)$ is $y_d(t)$, then the tracking error is $e_y(t) = y(t) - y_d(t)$.

Considering the system (10), the fractional order sliding surface is designed as,

$$s(t) = a_1 e_y(t) + a_2 D^\alpha e_y(t), \tag{27}$$

where a_1, a_2 are designed parameters, is the fractional order of the sliding surface. $\alpha \in (0, \beta)$ is different from the order of the system (10), and the good properties of fractional calculus can be applied into the sliding mode control.

According to the sliding surface and the system, the time derivative of (27) is

$$\begin{aligned}\dot{s}(t) &= a_1\dot{e}_y + a_2 D^\alpha \dot{e}_y \\ &= a_1\dot{e}_y + a_2 D^{1+\alpha-\beta}C(Ax + Bu + B_d d) - a_2 D^\alpha \dot{y}_d\end{aligned} \tag{28}$$

Setting $\dot{s}(t) = 0$, the equivalent control law can be calculated,

$$u_{eq}(t) = (CB)^{-1}\left(D^\beta y_d - \frac{a_1}{a_2}D^{-\alpha+\beta}e_y\right) - B^{-1}Ax - B^{-1}B_d\hat{d}. \tag{29}$$

In order to satisfy the sliding condition in the presence of the mismatched disturbances, the reaching law is

$$u_r(t) = (CB)^{-1}\left(-\frac{1}{a_2}D^{-1-\alpha+\beta}(k_1 s + k_2 sign(s))\right), \tag{30}$$

where k_1, k_2 are constant gains.

The fractional order sliding mode control law is

$$\begin{aligned}u(t) &= u_{eq}(t) + u_r(t) \\ &= (CB)^{-1}\left(D^\beta y_d - \frac{1}{a_2}D^{-1-\alpha+\beta}(k_1 s + k_2 sign(s)) - \frac{a_1}{a_2}D^{-\alpha+\beta}e_y\right) \\ &\quad - B^{-1}Ax - B^{-1}B_d\hat{d}.\end{aligned} \tag{31}$$

If the matrix B is invertible, we can use its inverse directly. Otherwise, we use the generalized inverse or pseudo-inverse of B when the matrix B is not singular.

Table 1
Quad-Rotor UAV system parameters.

Parameter	Value
K_{f_c}	$13.8N/V$
L_b	0.325m
L_f	0.325m
J_p	$0.9958\,\mathrm{kgm}^2$
J_r	$0.5531\,\mathrm{kgm}^2$
J_y	$1.5396\,\mathrm{kgm}^2$

Theorem 1. *For the general system (10), the fractional sliding order surface (27) and the controller (31), the closed-loop system is stable if $k_1 \ge 0$, $k_2 \ge a_2 B_d\zeta$. The output variable $y(t)$ can asymptotically track the reference $y_d(t)$ under the influence of the mismatched disturbance.*

Proof. The Lyapunov function is defined as

$$V = \frac{1}{2}s^2. \tag{32}$$

Based on (28), then the time derivative of (32) is

$$\begin{aligned}\dot{V} &= s\dot{s} \\ &= s(a_1\dot{e}_y + a_2 D^{1+\alpha-\beta}(C(Ax + Bu + B_d d) - D^\beta \dot{y}_d)) \\ &= s\left(a_1\dot{e}_y + a_2 D^{1+\alpha-\beta}\left(C\left(Ax + B\left((CB)^{-1}\left(D^\beta y_d - \frac{1}{a_2}D^{-1-\alpha+\beta}(k_1 s\right.\right.\right.\right.\right. \\ &\quad \left.\left.\left.\left.\left. + k_2 sign(s)) - \frac{a_1}{a_2}D^{-\alpha+\beta}e_y\right) - B^{-1}Ax - B^{-1}B_d\hat{d}\right) + B_d d\right) - D^\beta \dot{y}_d\right)\right)^{\cdot} \\ &= s(-k_1 s - k_2 sign(s) + a_2 B_d D^{1+\alpha-\beta}e_d) \\ &\le -k_1 s^2 - (k_2 - a_2 B_d D^{1+\alpha-\beta}e_d)|s|\end{aligned} \tag{33}$$

In the previous Section 3.1, $\|D^{1+\alpha-\beta}e_d(t)\| \le \zeta$ is proved by the proposed new fractional order disturbance observer (13). According to (33) and observer (13), if $k_1 \ge 0$, $k_2 \ge a_2 B_d\zeta$, $\dot{V} \le 0$, which implies that the sliding surface can be attained in finite time.

The reaching time is calculated in the following.

$$\begin{aligned}\dot{V}(t) &\le -k_1 s^2 - (k_2 - a_2 B_d D^{1+\alpha-\beta}e_d)|s| \\ \dot{V}(t) &\le -(k_2 - a_2 B_d\zeta)|s|\end{aligned}^{\cdot} \tag{34}$$

Taking the fractional integral α of (34) gives

$$D^{1-\alpha}V(t_r) - V(0)\frac{(t_r)^{\alpha-1}}{\Gamma(\alpha)} \le -(k_2 - a_2 B_d\zeta)D^{-\alpha}|s|, \tag{35}$$

where t_r is the reaching time.

Based on Lemma 1 and $V(t_r){=}0$, (35) is

$$\begin{aligned}&-V(0)\frac{(t_r)^{\alpha-1}}{\Gamma(\alpha)} \le -(k_2 - a_2 B_d\zeta)N \\ &(t_r)^{\alpha-1} \ge \frac{\Gamma(\alpha)(k_2 - a_2 B_d\zeta)N}{V(0)} \\ &\frac{1}{(t_r)^{1-\alpha}} \ge \frac{\Gamma(\alpha)(k_2 - a_2 B_d\zeta)N}{V(0)} \\ &t_r \le \left(\frac{V(0)}{\Gamma(\alpha)(k_2 - a_2 B_d\zeta)N}\right)^{\frac{1}{1-\alpha}}\end{aligned}^{\cdot} \tag{36}$$

Thus, the tracking error of output variables will converge to zero in finite time. □

For the integer order systems (11), the fractional order sliding mode control that we designed is still applicable. The formulation of FOSMC is

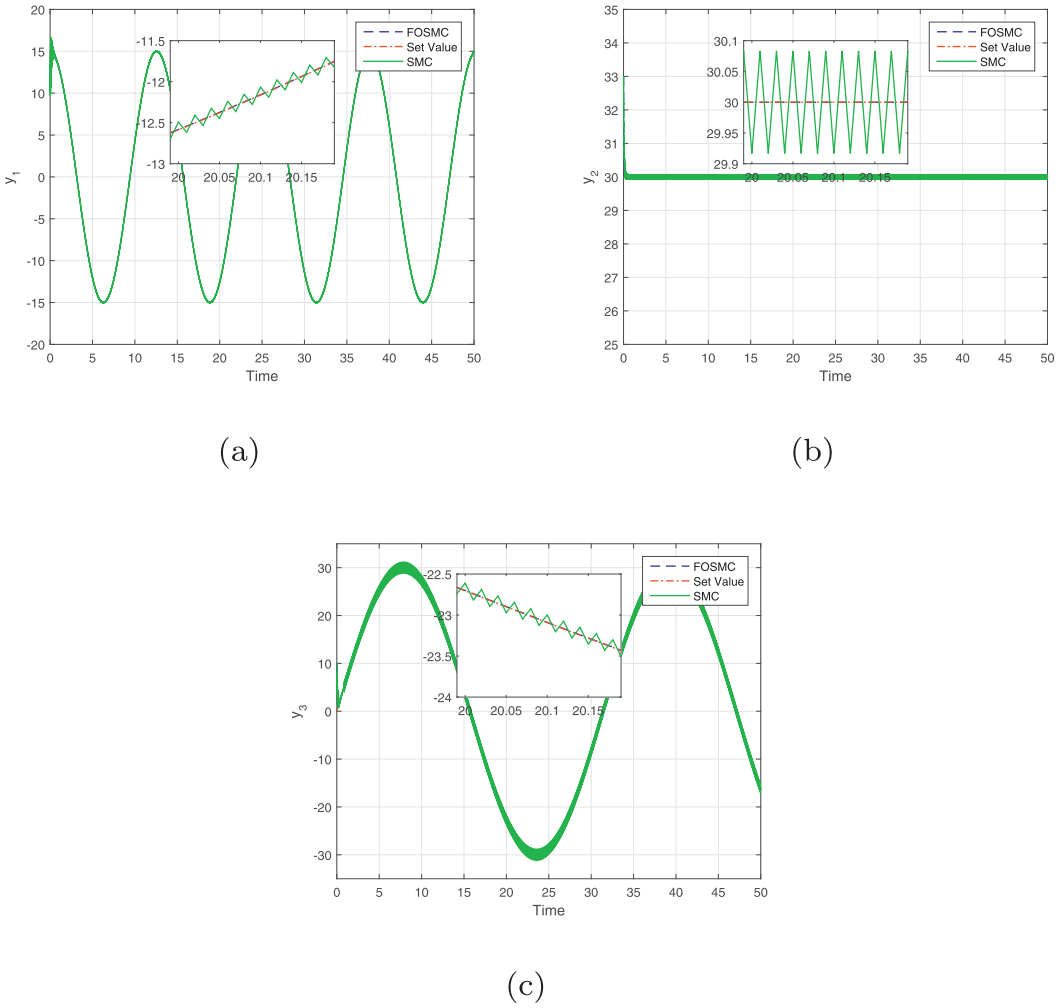

Fig. 1. Output response of FOSMC-DOB and SMC-DOB.

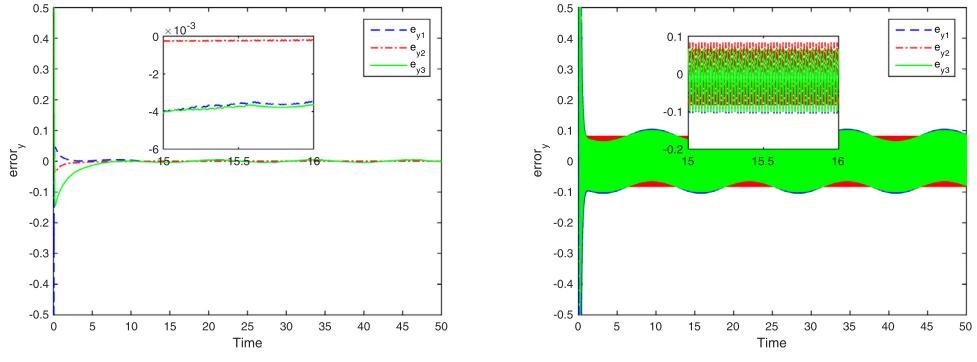

Fig. 2. Tracking errors of FOSMC-DOB and SMC-DOB.

Table 2
The sums of the squared errors of the tracking error.

Sum of squared errors	e_{y1}	e_{y2}	e_{y3}
FOSMC-DOB	0.6966	0.0311	0.4563
SMC-DOB	32.0930	29.6042	31.3324

$$s(t) = a_1 e_y(t) + a_2 D^{\alpha} e_y(t), \tag{37}$$

$$\begin{aligned} u(t) &= u_{eq}(t) + u_r(t) \\ &= (CB)^{-1}\left(\dot{y}_d - \frac{1}{a_2} D^{-\alpha}(k_1 s + k_2 sign(s)) - \frac{a_1}{a_2} D^{1-\alpha} e_y\right). \\ &\quad - B^{-1}Ax - B^{-1}B_d\hat{d} \end{aligned} \tag{38}$$

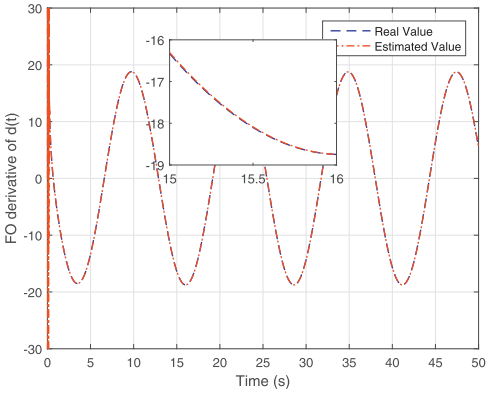

Fig. 3. Response curves of FOSMC-DOB.

Corollary 2. *For the general integer system (11), the fractional sliding order surface (37) and the controller (38), the closed-loop system is stable if* $k_1 \geq 0, k_2 \geq a_2 B_d \xi$. *The reaching time is*

$$t_r \leq \left(\frac{V(0)}{\Gamma(\alpha)(k_2 - a_2 B_d \xi) N} \right)^{\frac{1}{1-\alpha}}. \tag{39}$$

The integer order system can be viewed as a special case of the fractional order case. Thus the proof of Corollary 2 can be omitted.

4. Simulation results

To evaluate and verify the efficiency and excellent properties of the proposed FOSMC, two real systems are selected, namely Quad-Rotor Unmanned Aerial Vehicle(UAV) system and Maglev suspension system. First, we focus on the comparison of FOSMC and SMC, and the improvement of control effect for the integer order system. The attitude control of Quad-Rotor Unmanned Aerial Vehicle system is used for this simulation. Second, we demonstrate the good performance of the FOSMC and analyze the influence of sliding mode parameters on the control effect for the fractional order system. The Maglev suspension system is selected for this simulation. At the same time, for both two types systems, we demonstrate the good performance of the FOSMC method. We use the Oustaloup recursive filter and the modified version presented in [32] to evaluate fractional order differentiations. Generally speaking, Oustaloups approximation to fractional order operators are good enough in most cases. Then a MATLAB object FOTF toolbox is used to actualize the approximate calculation of FO differentiations and system simulations.

4.1. Simulation results of integer order systems

The attitude control of Quad-Rotor UAV system is an integer order system [35] which can be approximate described by

$$\begin{cases} \dot{x} = Ax + Bu + B_d d \\ y = Cx \end{cases}, \tag{40}$$

where $x = [p, r, y]^T$ presents pitch angle, roll angle, yaw angle, respectively. $u = [V_f, V_r, V_l, V_b]^T$ is the output of the motors. y is the output of angles. The state matrix, input matrix, disturbance matrix and output matrix A, B, B_d, C are given,

$$A = \begin{bmatrix} \frac{l_f K_1}{J_p} & 0 & 0 \\ 0 & \frac{l_f K_2}{J_r} & 0 \\ 0 & 0 & \frac{l_b K_3}{J_y} \end{bmatrix}, B = \begin{bmatrix} -\frac{K_{fc} l_f}{J_p} & \frac{K_{fc} l_f}{2J_p} & \frac{K_{fc} l_f}{2J_p} & 0 \\ 0 & \frac{\sqrt{3} K_{fc} l_f}{J_r} & -\frac{\sqrt{3} K_{fc} l_f}{J_r} & 0 \\ 0 & 0 & 0 & \frac{K_{fc} l_b}{J_y} \end{bmatrix},$$
$$B_d = [6 \;\; 0 \;\; 5]^T, C = \begin{bmatrix} 1 & 0 & 0 \\ 0 & 1 & 0 \\ 0 & 0 & 1 \end{bmatrix}. \tag{41}$$

The system parameters are listed in Table 1. The $K_i (i = 1, 2, 3)$ is approximately equal to zero and can be ignored when the UAV flies at low-altitude and low-speed.

Consider the tracking setting curves of output $y_d = [15\cos(0.5t) \;\; 30 \;\; 30\sin(0.2t)]^T$, disturbance $d = 35\cos(0.5t)$. The parameters of the controller and observer are listed as following: $a_1 = 6$, $a_2 = 16$, $k_1 = 28$, $k_2 = 6$, $\alpha = 0.9$, $L = [20 \;\; 1 \;\; 10]$. The simulation results are shown in Figs. 1 –5.

The controller is

$$\begin{aligned} u(t) &= u_{eq}(t) + u_r(t) \\ &= (CB)^{-1}\left(\dot{y}_d - \frac{1}{16} D^{-0.9}(28s + 6sign(s)) - \frac{3}{8} D^{0.1} e_y \right) - B^{-1} A x - B^{-1} B_d \hat{d}. \end{aligned} \tag{42}$$

The sliding surface is

$$s(t) = 6e_y(t) + 16 D^{0.9} e_y(t). \tag{43}$$

The tracking trajectory response of system states are shown in Fig. 1 (a)–(c). The tracking error of the two sliding mode control methods is expressed in Fig. 2. The setting curve of the output, the output curve with FOSMC-DOB and the output curve with integer order SMC-DOB are showed in red dash-dotted line, dotted blue line and green solid line, respectively. From the local enlarged figure, it is obvious that the FOSMC-DOB has better performances than the traditional integer order

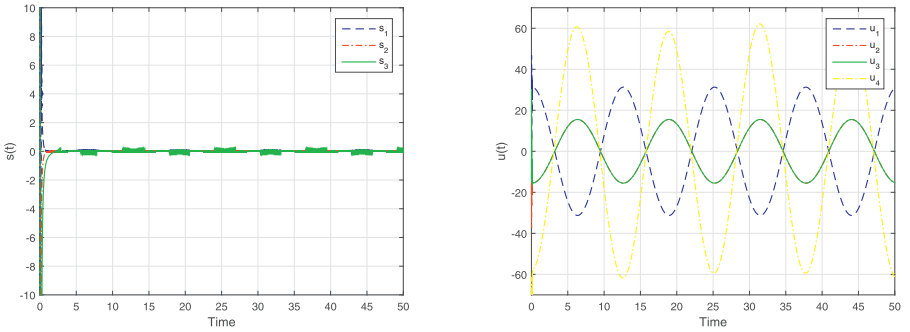

(a) FOSMC-DOB sliding surface (b) FOSMC-DOB control inputs

Fig. 4. Response curves of FOSMC-DOB.

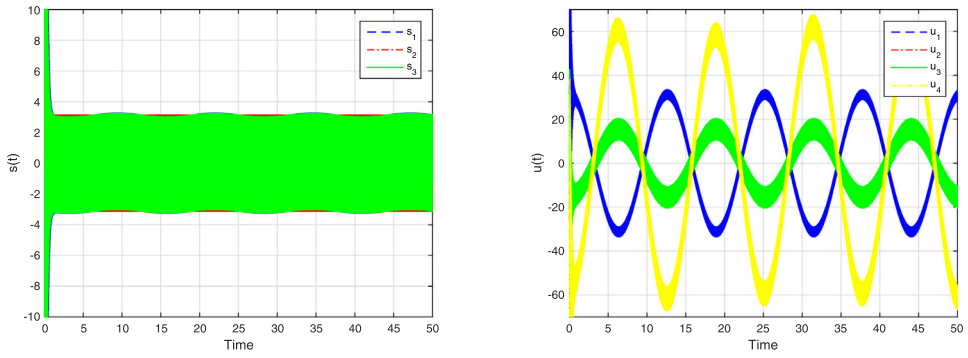

(a) SMC-DOB sliding surface (b) SMC-DOB control inputs

Fig. 5. Response curves of SMC-DOB.

Table 3
The reaching time (t_r) of SMC-DOB and FOSMC-DOB.

Sliding surface	s_1	s_2	s_3
FOSMC-DOB	0.75	0.7	1.4
SMC-DOB	1.5	0.7	1.45

Table 4
The parameters of Maglev suspension system.

Parameters	Definition	Value
A_p	Pole face area	0.01 m^2
I_0	Nominal current	10 A
G_0	Nominal air gap	0.015 m
L_c	Coils inductance	0.1
N_c	Number of turns	2000
R_c	Coils resistance	10 Ω
M_s	Carriage mass	1000 kg
K_b	Flux coefficient	0.0015 Tm
K_f	Force coefficient	0.0221 N/T^2

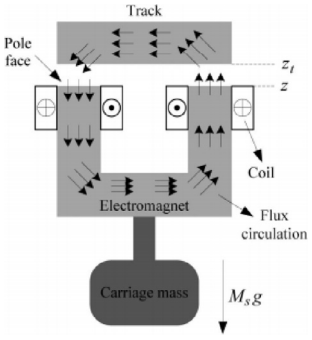

Fig. 6. The diagram of Maglev suspension system.

SMC-DOB for both fixed value tracking and curve tracking.The sums of the squared errors of the FOSMC-DOB and SMC-DOB tracking error is listed in Table 2. In order to evaluation the chattering, we ignore the violent dynamic process of the tracking error at the beginning, and the squared error in the stable domain is calculated from the fiftieth sampling points to the fifth thousand sampling points. Obviously, the chattering problem is well suppressed by FOSMC-DOB method compared with SMC-DOB method.

Fig. 3indicates that the real value and the estimated value of the fractional order derivative of disturbance. The dotted blue line represents the real value of the fractional order of external disturbance and the red dash-dotted line represents the estimated value of the fractional order of external disturbance. Regardless of the overall figure, or local zoom figure, we can see that the two curves almost coincide completely. Thus the fractional order derivative of the disturbance can be accurately estimated by the fractional order disturbance observer.

Furthermore, the Fig. 4 (a) and (b) show the curves of sliding surfaces and control inputs of FOSMC-DOB. The Fig. 5 shows the curves of sliding surfaces and control inputs of SMC-DOB. Compared Figs. 4 (b) and5 (b), four curves of different colors represent the output of different motors. Obviously, the chattering is weakened. The reaching time (t_r) of SMC-DOB and FOSMC-DOB are shown in Table 3. Thus the sliding surface can be attained in finite time. Meanwhile the reaching time of the FOSMC-DOB is shorter than SMC-DOB.

Figs. 1 –5 show the tracking trajectory, the accuracy of the disturbance estimates, as well as the reduction of chattering. All the results demonstrate the superiority of the proposed method from different perspectives. The proposed FOSMC-DOB has better control performance than the traditional SMC-DOB and the chattering problem is improved extremely. Meanwhile, the proposed fractional order disturbance observer can estimate the unmeasured mismatched disturbance very well.

4.2. Illustrative examples of fractional order systems

In order to verify the good performance of the proposed FOSMC-DOB method for a class of fractional order systems, the Maglev suspension system [31] is selected which is expressed as

$$\begin{cases} D^{\beta}x = Ax + Bu + B_d d \\ y = Cx \end{cases}, \tag{44}$$

where the state variables $x = [i, D^{\beta}z, (z_t - z)]^T$ represent the current, the vertical electromagnet and the air gap, respectively. The input $u = u_{coil}$ is the voltage, the disturbance $d = D^{\beta}z_t$ is the rail vertical velocity, the output variable $y = z_t - z$ is the variation of air gap. System matrices A, B, B_d, C are given,

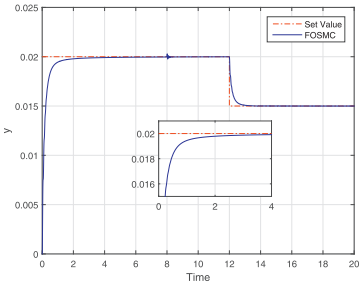

(a) Output response

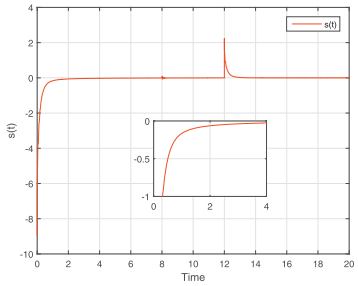

(b) FOSMC-DOB sliding surface

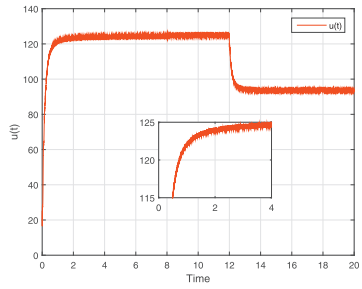

(c) Control signals of FOSMC-DOB

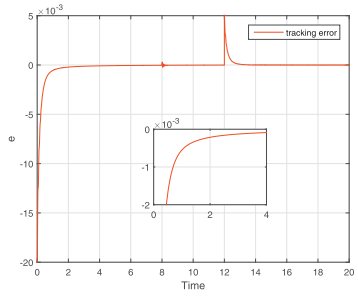

(d) Tracking error

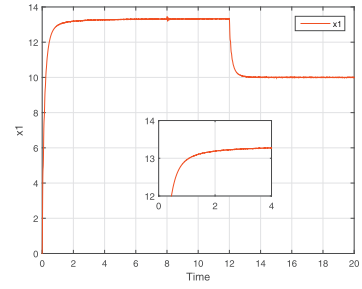

(e) State response x_1

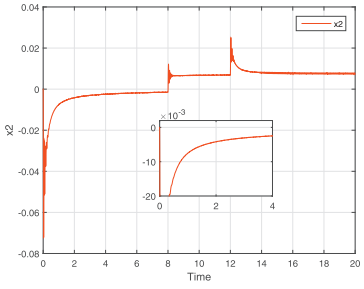

(f) State response x_2

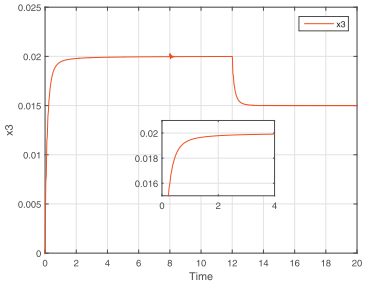

(g) State response x_3

Fig. 7. State response of Maglev suspension system.

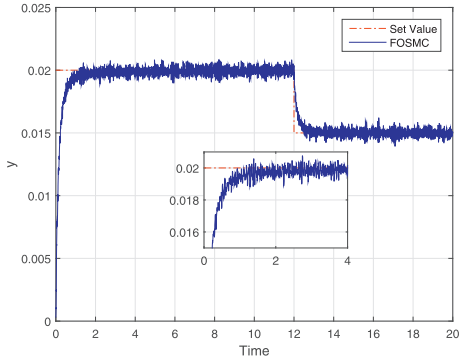

Fig. 8. Output response with 5% noise.

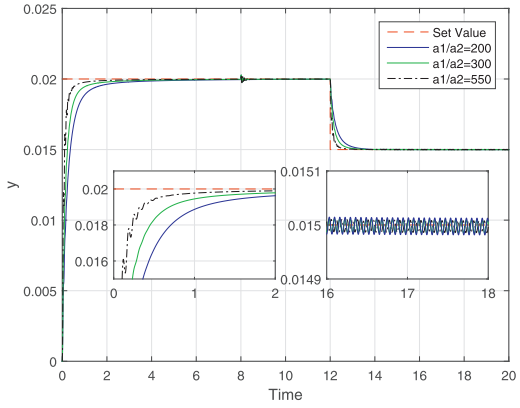

Fig. 9. Output responses with different parameters a_1/a_2.

Table 5
Sensitivity analysis of a_1/a_2.

a_1/a_2	k_1	k_2	t_s	e_{ss}
300	200	2	1.6	4.5×10^{-5}
550	200	2	0.8	1×10^{-5}
200	200	2	2.0	6.5×10^{-5}

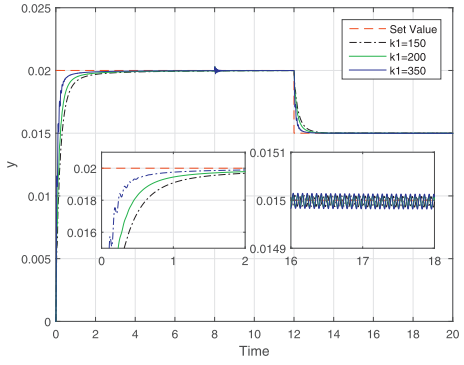

Fig. 10. Output responses with different parameters k_1.

Table 6
Sensitivity analysis of k_1.

a_1/a_2	k_1	k_2	t_s	e_{ss}
300	200	2	1.6	4.5×10^{-5}
300	350	2	0.6	1×10^{-4}
300	150	2	1.9	4×10^{-4}

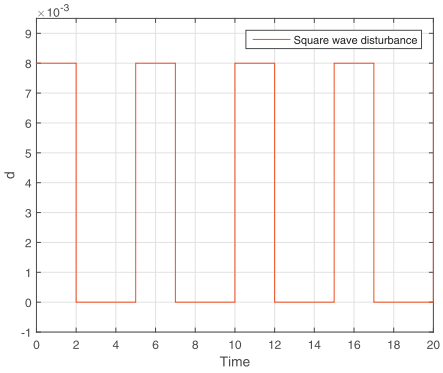

Fig. 11. The applied square wave disturbance on the Maglev suspension system.

$$A = \begin{bmatrix} \dfrac{-R_c}{L_c + K_b N_c \frac{A_p}{G_0}} & \dfrac{-K_b N_c A_p I_0}{G_0^2\left(L_c + K_b N_c \frac{A_p}{G_0}\right)} & 0 \\ -2K_f \dfrac{I_0}{M_s G_0^2} & 0 & 2K_f \dfrac{I_0^2}{M_s G_0^3} \\ 0 & -1 & 0 \end{bmatrix},$$

$$B = \begin{bmatrix} \dfrac{1}{L_c + K_b N_c \frac{A_p}{G_0}} \\ 0 \\ 0 \end{bmatrix},$$

$$B_d = \begin{bmatrix} \dfrac{K_b N_c A_p I_0}{G_0^2\left(L_c + K_b N_c \frac{A_p}{G_0}\right)} \\ 0 \\ 1 \end{bmatrix}, \; C = [0 \;\; 0 \;\; 1]. \tag{45}$$

The physical meanings and value of the parameters of Maglev suspension system are given in Table 4 [36]. The diagram of Maglev suspension system is shown in Fig. 6 [36].

The constraints for Maglev suspension system are listed as following: the maximum air gap deviation is less than 0.075 m, the maximum input coil voltage is less than 300 V, and the setting time is less than 3 s.

Consider the tracking target of output is 0.02 at the start, and changes to 0.015 in 12th second. In the 8th second a step external disturbance $d = 0.008$ is introduced. The parameters of the controller and observer are listed as following: $a_1 = 300$, $a_2 = 1$, $k_1 = 200$, $k_2 = 2$, $\alpha = 0.6$, $\beta = 0.7$, $L = [75 \;\; 0 \;\; 0]$.

The controller is

$$\begin{aligned} u(t) &= u_{eq}(t) + u_r(t) \\ &= (CB)^{-1}(D^{0.7} y_d - D^{-0.9}(200s + 2sign(s)). \\ &\quad - 300 D^{0.1} e_y) - B^{-1} A x - B^{-1} B_d \hat{d} \end{aligned} \tag{46}$$

The sliding surface is

$$s(t) = 300 e_y(t) + D^{0.6} e_y(t). \tag{47}$$

The simulation results of proposed FOSMC-DOB are depicted in Figs. 7–9.

According the response curves of the states, output, input and

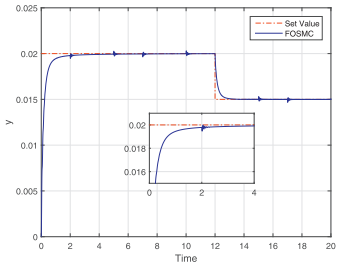

(a) Output response with square wave disturbance

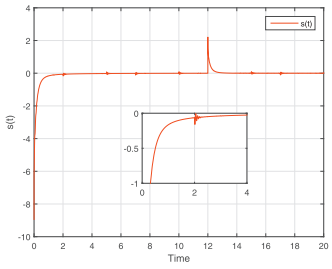

(b) FOSMC-DOB sliding surface with square wave disturbance

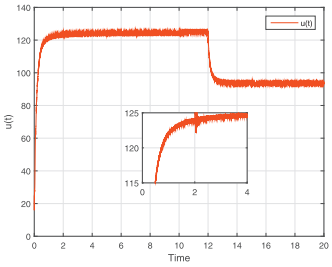

(c) Control signals of FOSMC-DOB with square wave disturbance

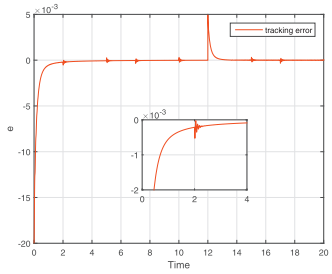

(d) Tracking error with square wave disturbance

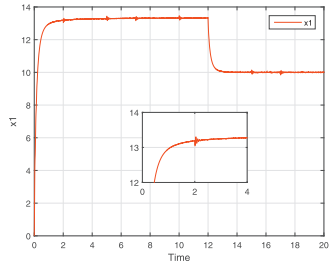

(e) State response x_1 with square wave disturbance

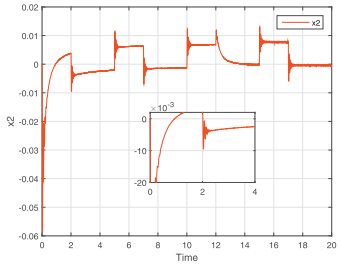

(f) State response x_2 with square wave disturbance

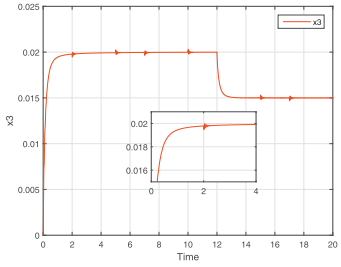

(g) State response x_3 with square wave disturbance

Fig. 12. State response of Maglev suspension system with square wave disturbance.

sliding surface shown in Fig. 7 (a)–(g), it is shown that the proposed FOSMC-DOB has excellent control performance. It satisfies the constraints of Maglev suspension system both in the dynamic and steady processes. It is obvious that this method has nice robustness to the mismatched disturbance from the 8th second of the curves. The good effect of tracking is achieved. It is embodied in the following parts. The response of system is very soon, steady tracking error is close to 0 and there is no overshoot. Moreover, the chattering problem is nearly eliminated. It is a great improvement for the sliding mode control method.

Fig. 8 shows the output response of the Maglev suspension system when the output signal has noises added in (5% noise).

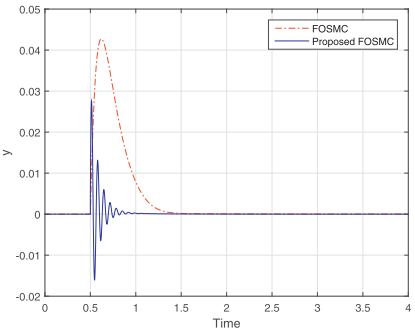

(a) Output response

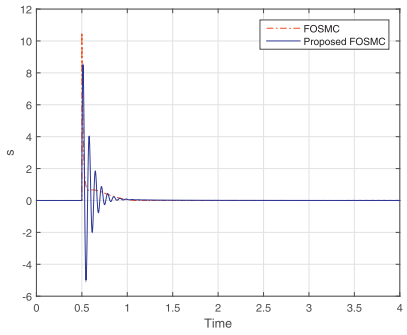

(b) FOSMC-DOB sliding surfaces

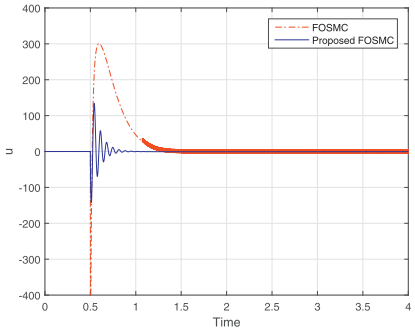

(c) Control signals of FOSMC-DOB

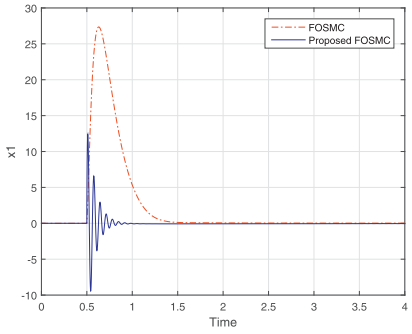

(d) State response x_1

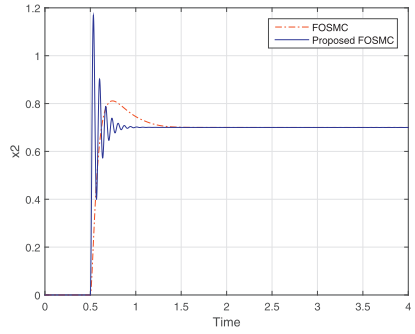

(e) State response x_2

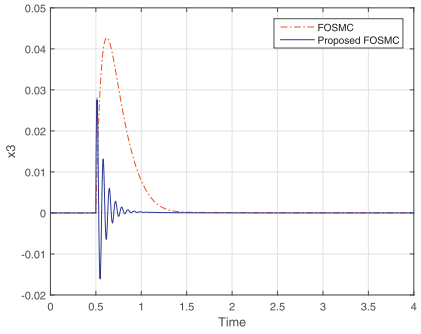

(f) State response x_3

Fig. 13. State response of Maglev suspension system with different FOSMC-DOB.

Fig. 9 shows the tracking performances of the output with different controller parameters a_1/a_2. This sensitivity analysis is tabulated in Table 5.

It can be seen from the simulation images that the setting time is shorter with a_1/a_2 decreases. However, in the transient process the chattering problem occurs, which is adverse for system. The steady-state error of the system is approximately unchanged. It is a good performance for real systems. In practice, we can make a balance between the setting time and the stationarity of transition process for a better control effect.

Fig. 10 and Table 6 analysis the sensitivity of k_1. It is indicate that if k_1 is larger, the setting time is shooter, but there is obvious chattering problem in transition process. It has similar performances with the changes of a_1/a_2.

Meanwhile, the changes of control effect is not obvious with different controller parameters a_1/a_2 and k_1. In all the cases of parameters variations, the tracking error is less than 0.5% and the chattering is almost avoided. We can adjust the controller parameters more conveniently and easily for a good control effect in real systems.

In addition, a square wave disturbance in Fig. 11 is applied on the FO-MAGLEV system. The simulation results are depicted in Fig. 12. The simulation results show that the square wave disturbance is also eliminated successfully using the proposed FOSMC-DOB.

Furthermore, a comparison between the proposed FOSMC-DOB and another FOSMC-DOB in paper [31] is simulated. The control parameters and the design details of the another FOSMC-DOB can be seen in paper [31]. After 0.5 s a step external disturbance $d = 0.7$ is applied. The simulation results are depicted in Fig. 13. The red dash-dotted line and the blue solid line represent the FOSMC in paper [31] and the proposed FOSMC-DOB respective. It can be observed that the two

methods can effectively eliminate the noise effect from the output of the system. Clearly, the proposed FOSMC-DOB has less overshoot and faster convergence speed than the FOSMC-DOB in paper [31]. However, there are some chattering effect at the beginning of the disturbance. Furthermore, the chattering of sliding mode motion can be eliminated by using the two methods.

The FOSMC-DOB in paper [31] focus on the stabilization and disturbance rejection for a class of fractional-order nonlinear dynamical systems with mismatched disturbances. The proposed FOSMC-DOB in this paper tries to make the output asymptotically tracking the desired reference in the finite time, and the tracking error approaching to zero without any effect from the external mismatched disturbances. So, the method in this paper is not very smooth in the transition process only at the aspect of disturbances rejection. But the proposed method is smooth enough for the tracking control of output as shown in Fig. 7.

5. Conclusion

In this paper, we propose a fractional order sliding mode control for a class of fractional order and integer order systems with mismatched disturbances. In order to estimate the external disturbance, we design a new fractional order disturbance observer. The proposed FOSMC-DOB makes the state and output quickly tracking the reference without any affection from the external mismatched disturbances. The applications in two different systems, the integer order UAV system and the fractional order Maglev suspension system, prove the versatility of the proposed method. The proposed FOSMC-DOB can decrease the tracking error at a high rate of speed and weaker chattering, compared with the traditional SMC-DOB. Moreover, the FOSMC-DOB is not sensitive with controller parameters.

References

[1] Kilbas AA, Srivastava HM, Trujillo JJ. Theory and applications of fractional differential equations. Elsevier; 2006.
[2] Ebaid A. Analysis of projectile motion in view of fractional calculus. Appl Math Model 2011;35(3):1231–9.
[3] Tepljakov A, Petlenkov E, Belikov J. Fopid controller tuning for fractional fopdt plants subject to design specifications in the frequency domain. European control conference.IEEE. 2015.
[4] Odibat ZM. Adaptive feedback control and synchronization ofnon-identical chaotic fractional order systems. Nonlinear Dyn 2009;60(4):479–87.
[5] Agrawal. A general formulation and solution scheme for fractional optimal control problems. Nonlinear Dyn 2004;38(1–4):323–37.
[6] Zhang X, Liu X, Zhu Q. Adaptive chatter free sliding mode control for a class of uncertain chaotic systems. Appl Math Comput 2014;232(232):431–5.
[7] Yin C, Chen YQ, Zhong SM. Fractional-order sliding mode based extremum seeking control of a class of nonlinear systems. Pergamon Press, Inc.; 2014.
[8] Yin C, Cheng Y, Chen YQ, Stark B, Zhong S. Adaptive fractional-order switching-type control method design for 3d fractional-order nonlinear systems. Nonlinear Dynam 2015;82(1):1–14.
[9] Han HC. Lmi-based sliding surface design for integral sliding mode control of mismatched uncertain systems. IEEE Trans Autom Control 2007;52(4):736–42.
[10] Kim K-S, Park Y, Oh S-H. Designing robust sliding hyperplanes for parametric uncertain systems: a riccati approach. Automatica 2000;36(7):1041–8.
[11] Utkin VI, Poznyak AS. Adaptive sliding mode control. vol. 440. Lecture Notes in Control & Information Sciences; 2013.
[12] Wang SW, Yu DW, Yu DL. Compensation for unmatched uncertainty with adaptive rbf network. Int J Eng Sci 2011;3(6):801–4.
[13] Gao Z, Liao X. Integral sliding mode control for fractional-order systems with mismatched uncertainties. Nonlinear Dyn 2013;72(1–2):27–35.
[14] Chen DY, Liu YX, Ma XY, Zhang RF. Control of a class of fractional-order chaotic systems via sliding mode. Nonlinear Dyn 2011;67(1):893–901.
[15] Chen Y, Wei Y, Zhong H, Wang Y. Sliding mode control with a second-order switching law for a class of nonlinear fractional order systems. Nonlinear Dyn 2016:1–11.
[16] Trigeassou JC, Maamri N, Sabatier J, Oustaloup A. A lyapunov approach to the stability of fractional differential equations. Signal Process 2011;91(3):437–45.
[17] Liang YW, Ting LW, Lin LG. Study of reliable control via an integral-type sliding mode control scheme. IEEE Trans Ind Electron 2012;59(8):3062–8.
[18] Cao W-J, Xu J-X. Nonlinear integral-type sliding surface for both matched and unmatched uncertain systems. IEEE Trans Autom Control 2004;49(8):1355–60.
[19] Aghababa MP. Design of a chatter-free terminal sliding mode controller for nonlinear fractional-order dynamical systems. Int J Control 2013;86(10):1744–56.
[20] Feng Y, Han F, Yu X. Chattering free full-order sliding-mode control. Automatica 2014;50(4):1310–4.
[21] Mobayen S. An adaptive chattering-free pid sliding mode control based on dynamic sliding manifolds for a class of uncertain nonlinear systems. Nonlinear Dyn 2015;82(1):1–8.
[22] Kim E. A fuzzy disturbance observer and its application to control. IEEE Trans Fuzzy Syst 2002;10(1):77–84.
[23] Chen WH, Ballance DJ, Gawthrop PJ, O'Reilly J. A nonlinear disturbance observer for robotic manipulators. IEEE Trans Ind Electron 2000;47(4):932–8.
[24] Oh Y, Wan KC, Oh Y, Wan KC. Disturbance-observer. IEEE Trans Mechatron 1999;4(2):133–46.
[25] Chen WH, Yang J, Guo L, Li S. Disturbance-observer-based control and related methodsan overview. IEEE Trans Ind Electron 2016;63(2):1083–95.
[26] Yang J, Li S, Yu X. Sliding-mode control for systems with mismatched uncertainties via a disturbance observer. IEEE Trans Ind Electron 2012;60(1):160–9.
[27] Li S, Yang J, Chen WH, Chen X. Disturbance observer-Based control: methods and applications. CRC Press, Inc.; 2014.
[28] Zhang J, Liu X, Xia Y, Zuo Z, Wang Y. Disturbance observer-based integral sliding-mode control for systems with mismatched disturbances. IEEE Trans Ind Electron 2016;63(11):7040–8.
[29] Wei Y, Tse PW, Yao Z, Wang Y. Adaptive backstepping output feedback control for a class of nonlinear fractional order systems. Nonlinear Dyn 2016;86(2):1–10.
[30] Mujumdar A, Kurode S, Tamhane B. Fractional order sliding mode control for single link flexible manipulator. IEEE international conference on control applications. 2013. p. 288–93.
[31] Pashaei S, Badamchizadeh M. A new fractional-order sliding mode controller via a nonlinear disturbance observer for a class of dynamical systems with mismatched disturbances. Isa T 2016;63:39–48.
[32] Monje CA, Chen YQ, Vinagre BM, Xue D, Feliu V. Fractional-order systems and controls. Springer London; 2010.
[33] Podlubny I. Fractional differential equations. Math Sci Eng; 1999.
[34] Walsh GC, Ye H, Bushnell LG. Stability analysis of networked control systems. IEEE Trans Control Syst Technol 2002;10(3):438–46.
[35] Lili L. Research on Modeling and control method of Quad-Rotor UAV systems. Master's thesis. Central South University; 2009.
[36] Michail K. Optimised configuration of sensing elements for control and fault tolerance applied to an electro-magnetic suspension system. Loughborough University. Ph.D. thesis; 2009.